Models of Human Normal Vocal Fold and Vocal Cord Nodule during Phonation

BENG 221
12/08/2016

Tianyi Lu, Lunan Shao, Su Xian

Table of Contents

Introduction

Vocal folds, which can also be called vocal cords, are consisted of two parts of mucous membrane and locate inside of the larynx [1]. They are at the top of trachea with the anterior end attached to the thyroid cartilage and the posterior end connected to the arytenoid cartilage [1]. An important function of vocal folds is phonation, which is processing of the air flow from the lung into audible sound [2]. During sound production, vocal folds, which are controlled by the vagus nerve, vibrate and cause the vibration in the air. This vibration on the vocal folds is composed by a mucosal wave that starts from the trachea side and moves upward in the direction of phonatory airflow [3].

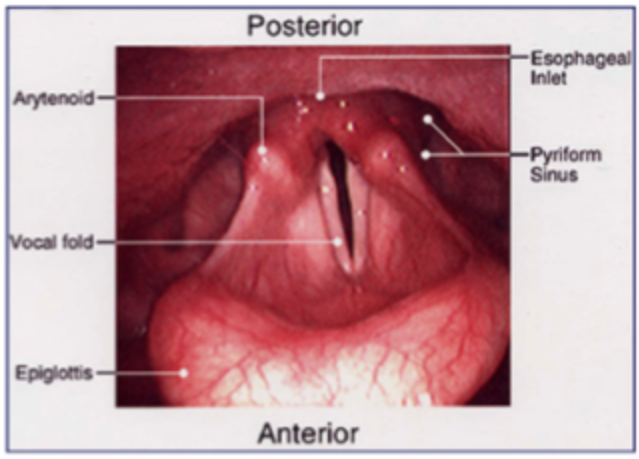

Figure 1. A Picture of Larynx. Adapted from website [4].

Vocal abuses, such as straining the vocal cords, may lead to a certain pathological case named vocal cord nodules, and this pathological case is specifically defined as small, benign growth on the vocal cords [5]. The symptom starts with soft, swollen spots on the vocal cords, which then become harder, and at last, the nodules may become larger and stiffer due to repeated vocal abuse[6]. The existence of the nodules results in changes in the quality and frequency of the voice[7]. The fundamental frequency, an acoustic measure of voice pitch, may stay normal, but the range of pitches that a person can produce may become smaller[7].

Figure 2. A Picture of Vocal Cord Nodules. Adapted from website [8].

This project is to model the vibration of both healthy and pathological vocal cords. Previously, Van den Berg stated that during phonation, the movement of the vocal folds can be described by the myoelastic aerodynamic theory[9]. According to this theory, negative Bernoulli pressure causes the vocal folds to close, resulting in a closed airspace under the glottis. When air pressure from the lung increases below the closed vocal folds, the folds are forced to open and release the air pressure. This lateral movement of the vocal folds continues until the natural elasticity of the tissue slows it down, and the vocal folds return to their initial, closed state[9].

However, according to Titze[10], the myoelastic aerodynamic theory does not cover all details in vocal folds vibration. He proposed a more elaborate body-cover model of vibration with a surface wave spreading along the cover. He stated that the driving force for vibration originates from the time delay in the vocal folds, which leads to a non-uniform movement on the superior and inferior end of the vocal folds. Based on Titze's results, this project intends to model the mucosal wave involved in vocal folds vibration[10].

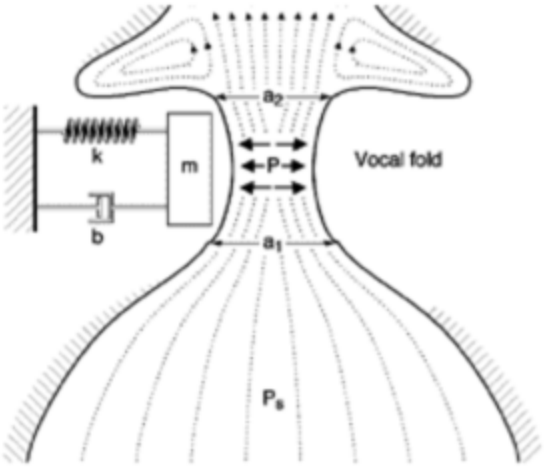

Figure 3. A Simple System from Myoelastic Aerodynamic Theory of Phonation. Adapted from website [11].

Problem statement

In previous literatures, there lacks a clear representation of the mucosal wave with respect to time and position in vocal fold vibration. Also, it remains unclear about the differences between the vibration pattern of normal focal cord and that of pathological one during phonation and the implications behind those differences. Last but not least, it remains uncertain how the differences in vibration pattern can contribute to the acoustic symptom in the vocal cord nodules. Therefore, this project aims to construct a wave function model to approximate the vocal cord vibrations in both cases through using Matlab, and it will analyze the power spectral density in Fourier domain of the vibration to deduce the frequency change under pathological conditions.

Assumptions

- It is assumed that the vocal folds are homogeneous materials, which have uniform

composition and uniform properties.

- Since the vocal fold vibration amplitude is relatively small compared to the scale of vocal cords, the vibration waves in vocal cord can be described by a one-dimensional wave function.
- The vibration in Y-direction is negligible compared to Z-direction, which is not only consistent with the fine structure of the surface layer but also complies with airflow along Z-direction.
- In pathological case, nodule formation only affects the density of the tissue but merely changes the shape.

Method

The vocal cord surface vibration is governed by continual mechanics. By assuming homogeneity of material property and regular geometry, the governing kinematic equation of the surface can be simplified to wave equation with wave velocity being 94 cm/s in normal condition [12]. To simulate the vibration of the vocal cord, it becomes equivalent to solving the wave equation with proper parameters and meaningful boundary and initial conditions(IC). In this project, the IC is set as zero position value and zero position gradient, which is reasonable in that before vibration the vocal cord can be assumed flat and static. The boundary condition (BC) is more difficult to set because the vocal cord is a live biological tissue which can be irregular in geometry and properties. For simplicity, the region of scope is set to be a square area lying vertically along the direction of airflow; for each point in this region, the wave equation gives the value of the position, which is measured as the distance between the surface of the vocal cord and the middle line of the air pathway; the lower boundary – the bottom of the vocal cord where air from trachea flows in – is set to vibrate horizontally in a sine pattern at 100 Hz, the range of which is 0-0.125 cm; the front and back boundaries are set to be zero gradient in horizontal direction; the upper boundary of the region is set to be zero gradient [12]. This setup of boundaries models a vibration at 100 Hz caused by airflow, featuring the center region of the vocal cord that can be assumed as a 1D wave motion in the direction of the airflow; the amplitude of vibration is constrained by the maximum opening width of the vocal cord 0.25 cm [10]. After simulating 1D wave pattern, a 2D wave pattern is tested out by featuring the whole half side of the vocal cord, with front and back boundaries set to be zero values because in this condition, the front and back boundaries are the lines where the two sides of the vocal cord connect and should be assumed static. The pathological conditions under nodules and polyps are modeled as tissue density changes, which then alters the wave velocity in the governing equation. The density change is manipulated as percentage changes.

The solution in time and space is obtained as a numerical solution using PDE toolbox in Matlab. To compare between 1D and 2D models, the problem is solved using FEM. The results to obtain are animations of the motions in surface plots and the waveforms of the vibrations at the upper boundary. To understand the waveforms, the waveforms of the position value are transformed into power density which is proportional to square of position value and the power density values are further processed as normalized power density values in frequency domain after discrete Fourier Transformation, so that the power density distribution of the waveforms in frequency domain can be compared among different pathological conditions. Since the time step of the numerical solution is 1ms, the sampling frequency of the data is assumed as 1 kHz. The simulation is run for 0.5 second in general.

Model

Governing Differential Equation:

$$\rho \frac{\partial^2 u}{\partial t^2} = T \nabla^2 u$$

$c = \sqrt{T/\rho}$, c=94 cm/s under normal condition

Finite Element Method to obtain numerical solution:

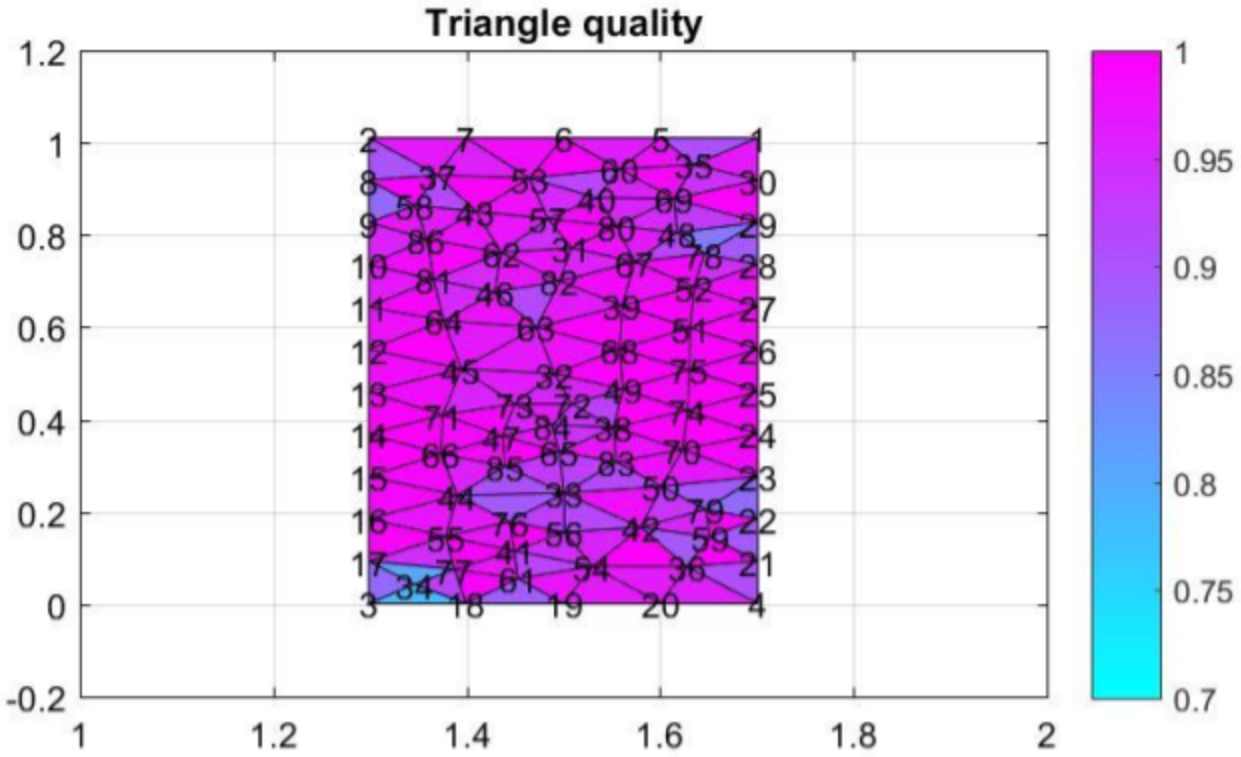

Figure 4. FEM Mesh of the Central Vocal Cord Region.

Results

The simulated vocal cord vibration under healthy conditions turns to be smooth and periodic, which is similar to reality. A full animation of the model for 0.5 second is demonstrated at the presentation and will be attached to this report. Figure 5 captures a characteristic moment in the animation.

To further inspect the behavior of the model, we zoomed in at the upper boundary (z=1 cm) and analyzed the waveform of vibration at this point. Figure 6 demonstrates the vibrational

waveform at the upper boundary of the model. The waveform shows an oscillatory pattern with a controlled small amplitude, which matches the description in Titze's results [10].

Due to the complexity of the waveform, it is difficult to recognize highly informative pattern by merely looking at the waveform plot. Thus, an advanced analysis in Fourier domain is performed to obtain power density spectrum. In Figure 7, the power density spectrum of low frequency region (0-200 Hz) shows 5 peaks distributed sparsely between 0 and 100 Hz, with relatively close power densities.

The growth of vocal cord nodules is modeled by tissue density increase. The animation of the vocal cords with nodules shows little difference compared to healthy vocal cords vibration but merely a slower wave velocity and higher amplitude. Therefore we proceeded to analyze the vibration waveform at the upper boundary.

Figure 8 shows a clear trend of increasing peak with increasing tissue density. For an increase of tissue density within 10%, the peak of the vibration is relatively unchanged, indicating a controlled vibration. When tissue density increases to 23%, the peak increases over 0.3 cm. An increase of tissue density to 38% results in a peak position value of 2 cm. Accompanied with increasing peak, clustering of waveforms is also observed. In Case A and B, the waveforms contain scattered peaks; in Case C, the waveform shows heavily condensed peaks, which we call clustering behavior of increasing tissue density; in Case D, the peaks are so clustered that the result looks like a growing cone, which is observed only at high tissue densities, i.e. 38%.

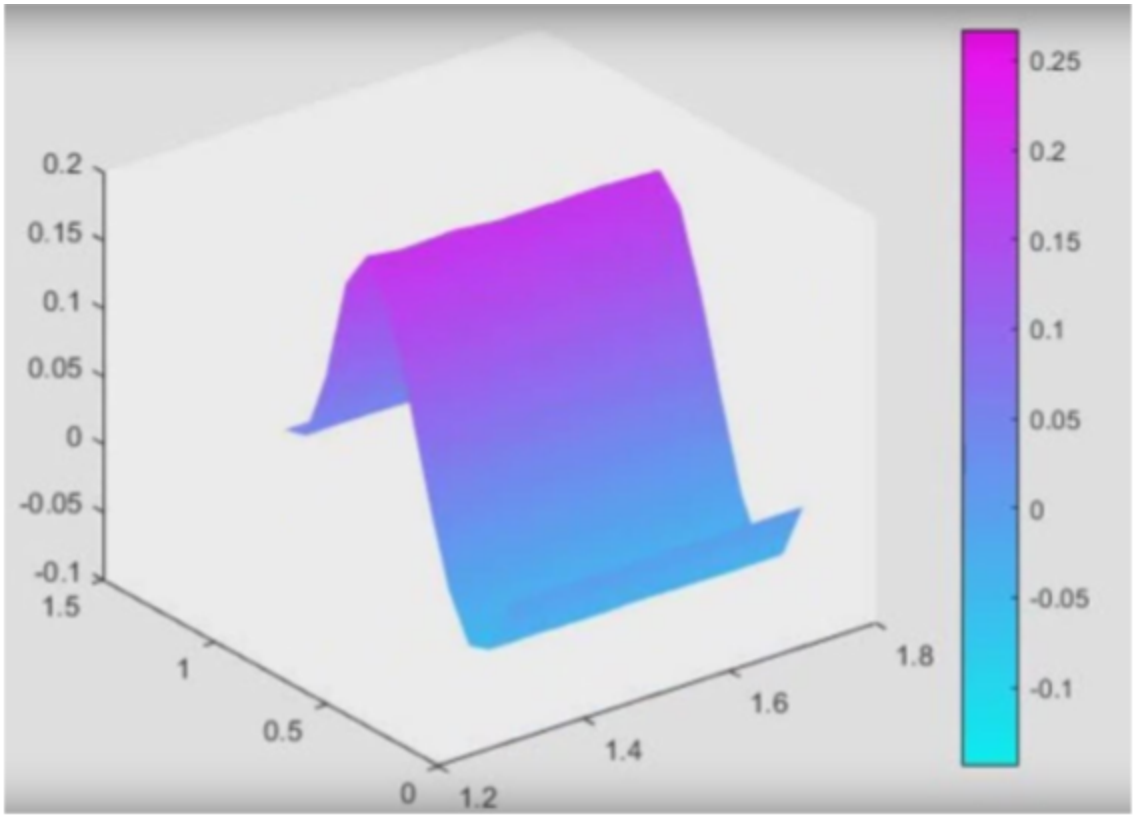

Figure 5. Surface Plot of the Vibration of Healthy Vocal Cords

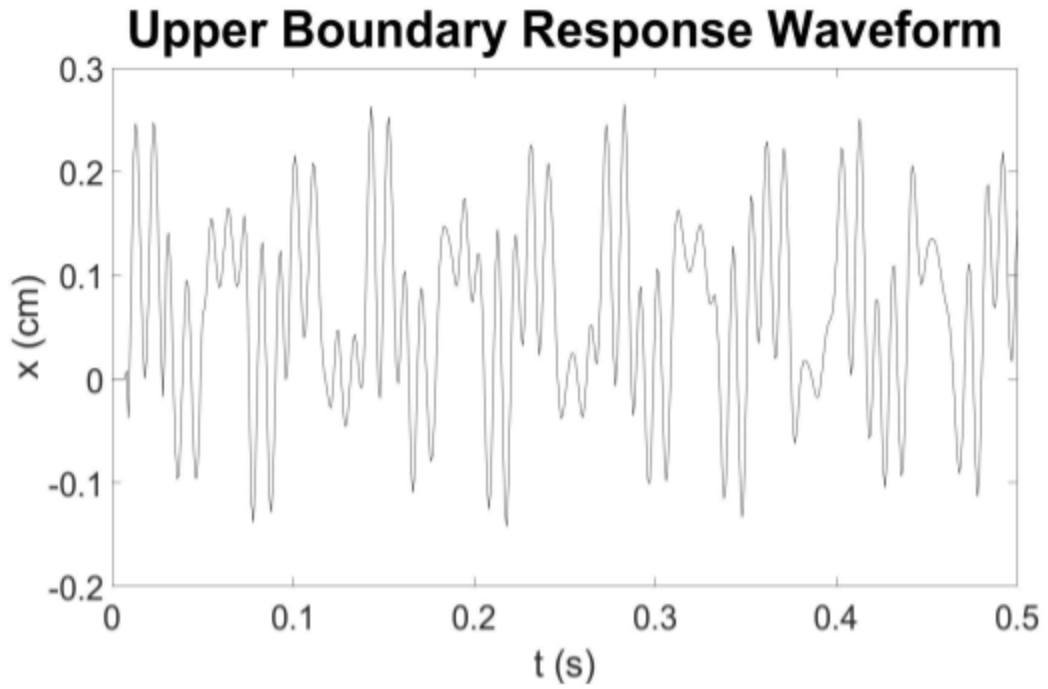

Figure 6. Vibration at the Upper Boundary of Healthy Vocal Cords.

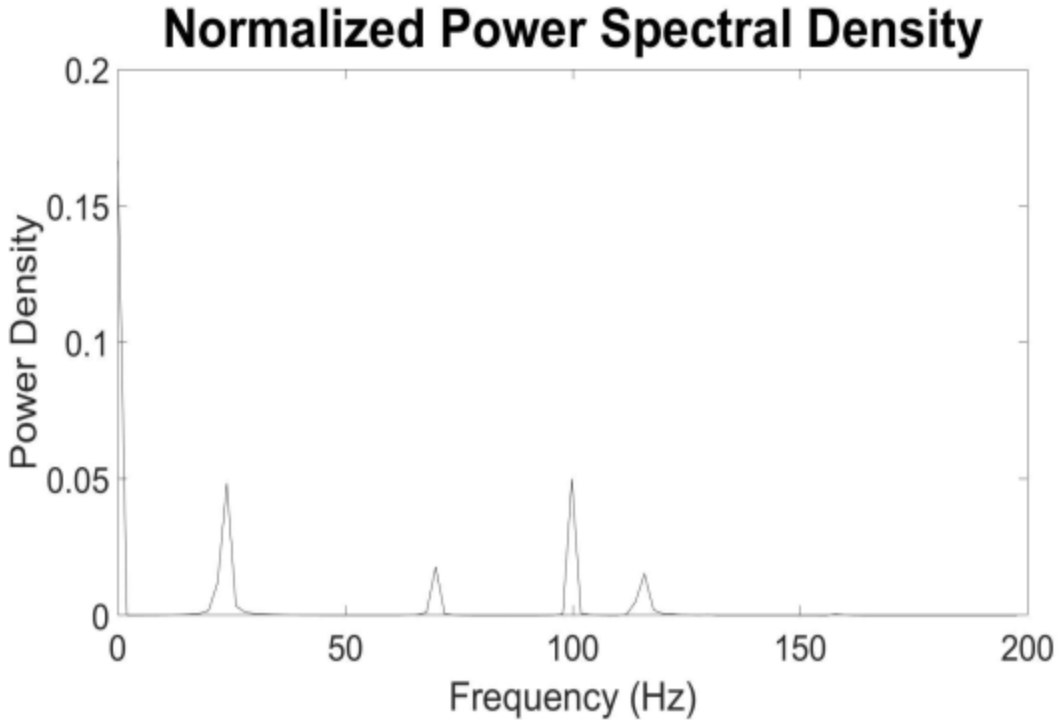

Figure 7. Normalized Power Spectral Density of Healthy Vocal Cords

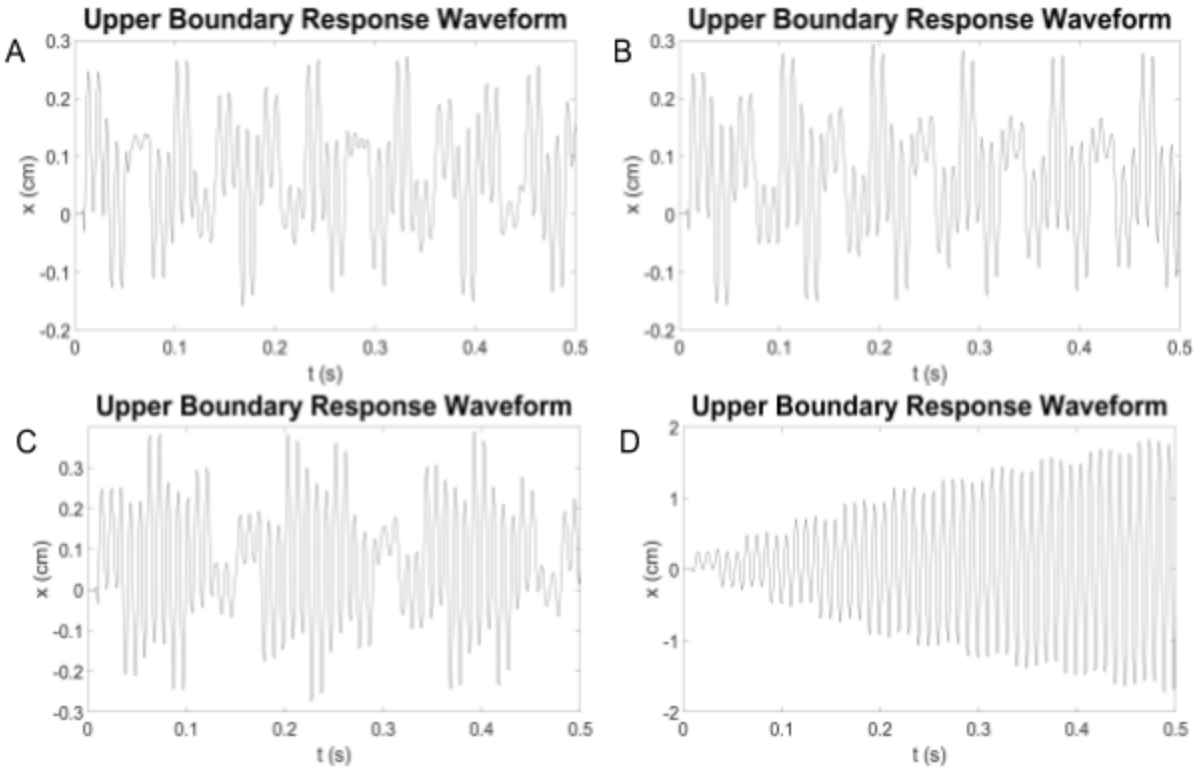

Figure 8. Vibration at Upper Boundary under Pathological Conditions. Tissue density increase A: 6%; B: 11%; C: 23%; D: 38%

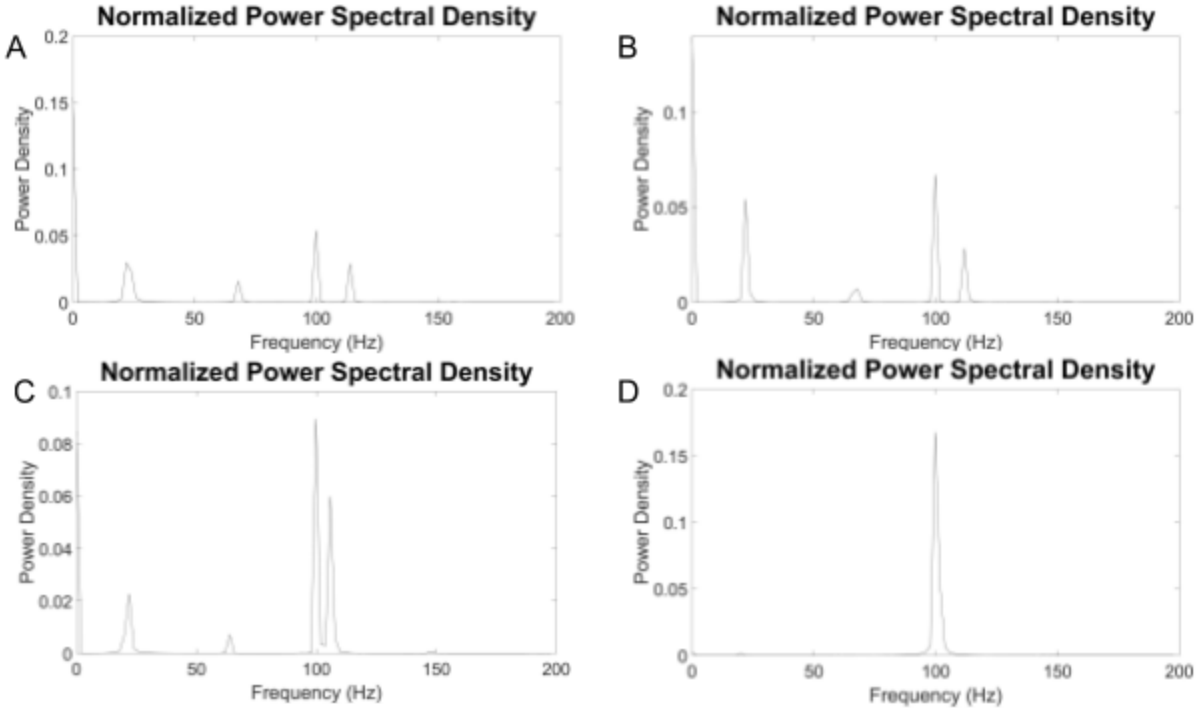

Figure 9. Normalized Power Spectral Density under Pathologic Conditions. Tissue density increase A: 6%; B: 11%; C: 23%; D: 38%

Figure 9 shows frequency distribution of power density. Compared with the power density spectrum of healthy conditions, it can be concluded that as tissue density increases, the peaks of power density shifts towards the peak of 100 Hz, featuring aggregation of peaks in power density spectrum; in a simpler way to say, as tissue density increases, the power density of 100 Hz increases while power density of other frequencies decreases. Therefore it is reasonable to suspect that the power density of 100 Hz could be an indicator of tissue density increase.

To visual the shift of peaks in power spectral density, Figure 10 is made featuring the distribution of power densities under normal condition, 11% tissue density increase and 23% tissue density increase. It clearly shows that peak at 100 Hz shifts up and other peaks shift down; in addition, the small peak to the right of 100 Hz tends to shift left and shift up to merge with the peak of 100 Hz as tissue density increases, which becomes obvious in Figure 9 Case D, where the two peaks completely merge into one large peak, surpassing other peaks dominantly. To correlate this feature with tissue density, the percentage of the power density near 100 Hz is plotted against tissue density and is captured in Figure 11.

In Figure 11, the 100 Hz power density percentage fits well with a smooth curve for tissue density increase up to 25%; for tissue density increase higher than 25%, the fitted curve is not as smooth, indicating that the fitting is most suited under 25% tissue density increase.

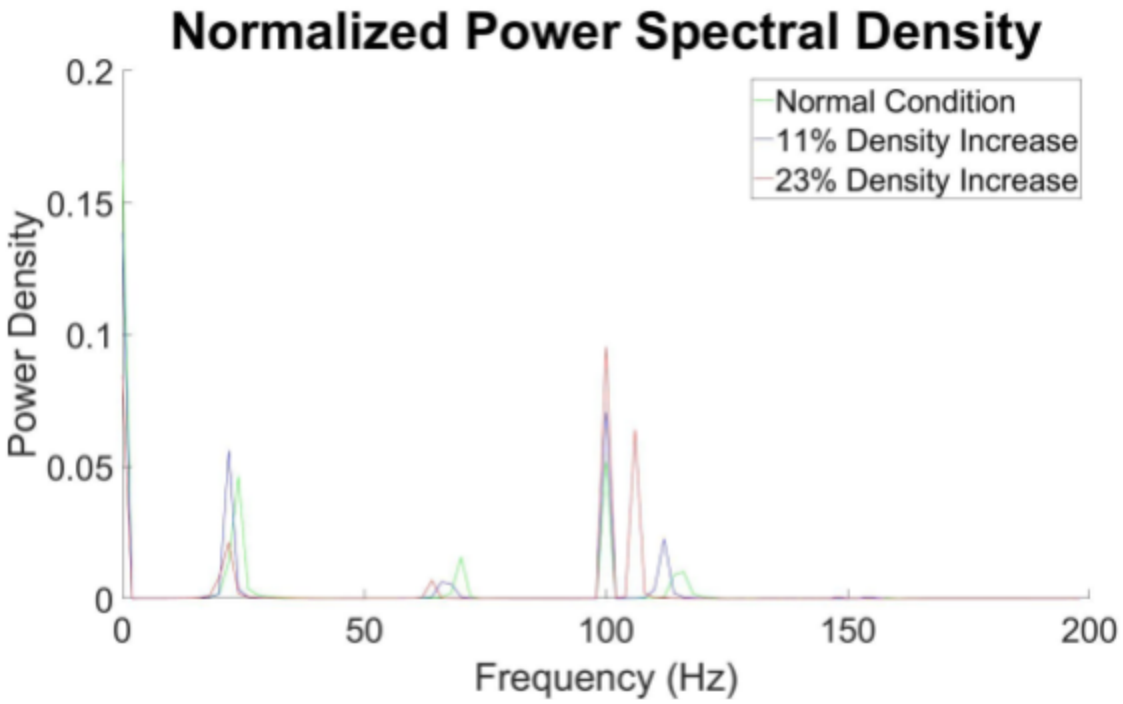

Figure 10. Power Density Pattern Comparison. Tissue density is increased 0% (normal condition) in green, 11% in blue, 23% in red.

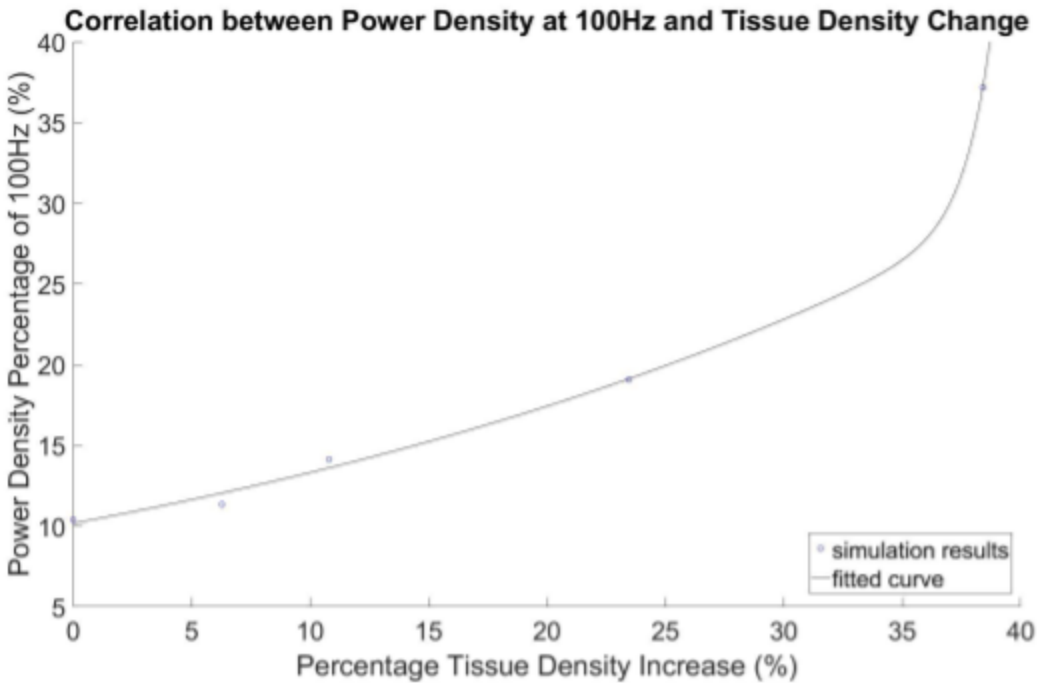

Figure 11. Correlation between Power Density Percentage at 100 Hz and Tissue Density Change

A

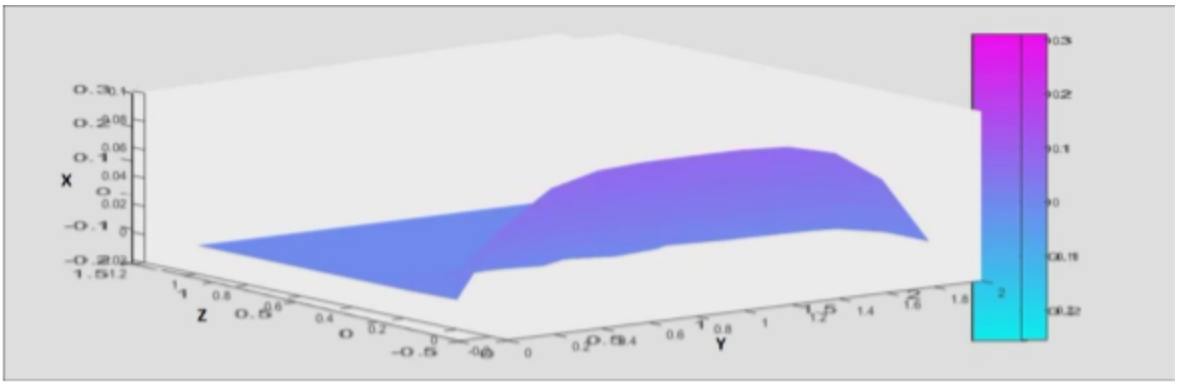

B

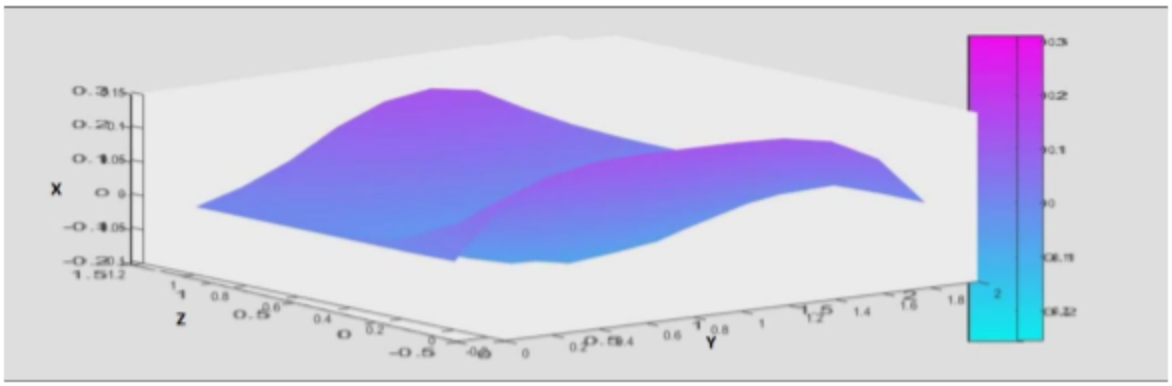

Figure 12. Surface Plots of the 2D Model. A: The initiation state of vibration. B: Mucosal wave propagation

The 2D model of vocal cords vibration is an expansion of the model. The 2D model features the full vertical half-side of the vocal cords. This model takes Y-direction vibration into account. The results shown in Figure 12 demonstrates how mucosal wave is initiated by lower boundary vibration and propagates in both Y and Z directions.

Discussion

The animation is a good way to represent how the mucosal wave propagates on the vocal cords in response to lower boundary vibrations. The wave-pattern shown in Figure 5 matches up well with reality visually. However, due to the fast frequency and complicated vibrational patterns, merely looking at the animation would not yield informative conclusions regarding pathological conditions. Therefore, the vibrational patterns at the upper boundary are investigated in this project.

The waveform of the upper boundary was analyzed to show a pathologic difference between healthy condition. In Figure 6, under healthy conditions the peak of waveform stays around 0.25 cm, representing well-controlled status. From Figure 8, when tissue density was increased over 23%, the peak value of waveform is about to exceed 0.3 cm, which is the limitation of waveform peak [11]. Evident clustering formation also starts at 23% of tissue density increase. When tissue density is increased to 38%, the waveform is significantly different and the peak goes over 2 cm, being highly unrealistic. This phenomenon indicates that this model is suitable for a tissue density increase within 23%. In this range the waveform provides some difference in pathologic conditions compared with healthy conditions, but the waveform by itself is not conclusive enough.

The analysis of power density in healthy conditions shows a sparse distribution between 0 Hz to 100 Hz and this distribution shifts towards 100 Hz in pathologic conditions, which latter becomes the dominant frequency when tissue density is increased by 38%. The frequency aggregation at 100 Hz actually matches well with a clinical reports stating a reduced frequency distribution in pathologic conditions [12]. One of the symptoms of vocal cord nodules also features a reducing range of the frequency [13]. The narrowing-down trend of frequency displayed some fundamental frequency loss in pathologic conditions compared to healthy conditions, which coincides with the symptoms of vocal cord nodules. The plot of percentage power density at 100 Hz also turns out to correlates with tissue density increase within 25% monotonically. Therefore this correlation quantitatively depicts the common symptom of vocal cord nodules.

However the clear correlation between the percentage power density at 100 Hz and tissue density is not so reasonable for tissue density increased by over 30% because after 30%, the percentage power density curve starts to rise drastically. This finding matches previously described limitation (waveform is reasonable within 23% tissue density increase). Thus both analysis points out that this model is applicable for tissue density increase within 23%.

What is significant with this model is that the correlation could potentially be used to diagnose the severity of vocal cords impairment. Because growth of nodules would increase the tissue density, this correlation between percentage of power density at 100 Hz and tissue density increase could directly correlate power density distribution to growth of nodules.

Limitations

In order to apply the wave equation to simulate vocal cords vibration, it is assumed that the tissue is uniform and homogeneous. However, in reality, the mechanical properties of vocal cords vary upon different area even though this variation may be slight. Therefore, this assumption may lead to some discrepancies in this model when it is compared to the actual vibration of the vocal folds. Another limitation is that a simple sine function with an amplitude of 0.125 cm is set for the lower boundary condition to serve as the initiation of vibration caused by air pressure from the lung. However, the relationship between lung pressure and lower boundary vibration could be much more complex in the reality. In addition to these limitations, in pathologic model the size of nodules growing on the vocal cords is assumed to be negligible so that the boundary condition is still the same as in the healthy model, but in real situation the size of nodules may vary and could be large, whose impact on geometry of the vocal cords is not negligible. As a result, for large nodules, this model may not apply any more. To obtain a more accurate model, the BC and IC in this model must be modified to incorporate how nodules change the geometry.

Conclusion

In sum, using wave equation to model the vocal cords vibration and to analyze what happens in pathologic situation turns out effective. In the healthy conditions, this model gives out the vibrational waveform of vocal cords that fits well with reality featuring controlled amplitude and reasonable frequency distribution.

The pathologic model yields a slower vibration with increased amplitude which also matches real situation.By analyzing the vibrational waveform at upper boundary with increasing tissue density, it can be concluded that the vocal cords vibration under nodules conditions features cluster formation, out-of-range amplitude increase and decrease in range of frequency distribution. The results also indicate that the appropriate scope of inspection for this model is within 23% increase in tissue density.

In clinical situations, the correlation of tissue density and power density percentage at 100 Hz implicates a method to diagnose the severity of nodules by frequency analysis of mucosal wave. By obtaining the power density of 100 Hz from measurements of mucosal waveforms in patients, researchers could potentially analyze the severity of nodules such as size and mass. A promising method would be placing a motion detector close enough to the vocal cords to record the waveform of upper vocal cords during phonation and finding the power spectral density in Fourier domain.Subsequently, by calculating percentage of power density at 100 Hz, the change of tissue density can be inferred. However, to develop a clinical diagnostic method, more clinical experiments are required to verify and append to the correlation found in this paper.

Future Investigations

In this project, many assumptions are made to simplify this model and eventually solve it numerically. However, under real physiological circumstances, the model has to include some key features that are omitted in this paper to achieve higher accuracy. First of all, the boundary condition at the inferior end has to be modified to be realistic. In order to find the realistic BC, it is necessary to obtain a pressure-wave relationship and to include the pressure profile at the inferior end of the vocal cord. Furthermore, even though the vibration in the Y-direction is small,

it will still be included in the more realistic model. Then, in the future work, it will be good to take the dimensions of the nodules into the consideration and integrate this factor into the model by modifying the geometry. Lastly, the model will need to include inhomogeneous material properties by modifying wave velocity to a function of Y and Z locations. Therefore, the attempt of 2D modeling in Figure 12 is not significantly relevant since expansion of 1D wave model into 2D wave model requires much more complicated modifications.

Reference

1. Vashishta, Rishi. "Larynx Anatomy ." *Larynx Anatomy: Gross Anatomy, Functional Anatomy of the Larynx, Laryngeal Tissue*. N.p., n.d. Web. 09 Dec. 2016.
2. "Types of Phonation." Types of Phonation. N.p., n.d. Web. 09 Dec. 2016.
3. Mau, Ted, et al. "Modulating phonation through alteration of vocal fold medial surface contour." *The Laryngoscope* 122.9 (2012): 2005-2014.
4. "Voiceproblem.org." *Voiceproblem.org - voiceproblem Resources and Information.* N.p., n.d. Web. 09 Dec. 2016.
5. Lancer, Jack M., et al. "Vocal cord nodules: a review." *Clinical Otolaryngology & Allied Sciences* 13.1 (1988): 43-51.
6. "Vocal Cord Nodules and Polyps." *American Speech-Language-Hearing Association*. ASHA, n.d. Web. 09 Dec. 2016.
7. Casper, Janina K., and Rebecca Leonard. *Understanding voice problems: A physiological perspective for diagnosis and treatment*. Lippincott Williams & Wilkins, 2006.
8. "Voice and Swallowing." *ENT and Allergy Associates | Voice and Swallowing*. N.p., n.d. Web. 09 Dec. 2016.
9. Van den Berg, Janwillem. "Myoelastic-aerodynamic theory of voice production." *Journal of Speech, Language, and Hearing Research* 1.3 (1958): 227-244.
10. Titze, Ingo R. "The physics of small-amplitude oscillation of the vocal folds." *The Journal of the Acoustical Society of America* 83.4 (1988): 1536-1552.
11. "The National Center for Voice and Speech - Tutorials." *The National Center for Voice and Speech - Tutorials*. N.p., n.d. Web. 09 Dec. 2016.
12. Story, Brad H., and Ingo R. Titze. "Voice simulation with a body-cover model of the vocal folds." *The Journal of the Acoustical Society of America* 97.2 (1995): 1249-1260.
13. Verdolini, Katherine, et al., eds. *Classification manual for voice disorders-I*. Psychology Press, 2014.

Appendix

plotting.m

```
figure(1)
hold on
P0=spect(u(6,:),500,1000,100,'g',1,2);
P5=spect(u_95(8,:),500,1000,100,'b',1,3);
P10=spect(u_90(8,:),500,1000,100,'r',1,4);
figure(1)
legend('Normal Condition','11% Density Increase','23% Density Increase')
P0=spect(u(6,:),500,1000,100,'k',2,3);
P3=spect(u_97(8,:),500,1000,100,'k',4,5);
P5=spect(u_95(8,:),500,1000,100,'k',6,7);
P10=spect(u_90(8,:),500,1000,100,'k',8,9);
P15=spect(u_85(8,:),500,1000,100,'k',10,11);
pct_0=2*P0(51);%2Hz is step length in fft
pct_3=2*P3(51);
pct_5=2*P5(51);
pct_10=2*P10(51);
pct_15=2*P15(51);
pct=[pct_0,pct_3,pct_5,pct_10,pct_15];
pct=pct';
pct=pct*100;
xpct=[1,0.97,0.95,0.9,0.85];
xpct=1./(xpct.^2);
xpct=(xpct-1)*100;
xpct=xpct';
figure()
hold on
scatter(xpct,pct,'bo')
set(gca,'fontsize',30);
p=fit(xpct,pct,'exp2');
plot(p,'k')
xlabel('Percentage Tissue Density Increase (%)')
ylabel('Power Density Percentage of 100Hz (%)')
title('Correlation between Power Density at 100Hz and Tissue Density Change')
axis([0 40 5 40])
legend('simulation results','fitted curve')
```

spect.m

```
function spect(z,n,rate,dis,clr,num1,num2)
Z=fft(z,n);
pwr=Z.*conj(Z)/n;
```

```
pwr=pwr/sum(pwr)/(rate/n);
f=rate/n*(0:(dis-1));
figure(num1)
plot(f,pwr(1:dis),clr)
set(gca,'fontsize',40);
xlabel('Frequency (Hz)')
ylabel('Power Density')
title('Normalized Power Spectral Density','FontSize',60)
figure(num2)
t=0:0.001:0.5;
plot(t,z,clr)
set(gca,'fontsize',40);
xlabel('t (s)')
ylabel('x (cm)')
title('Upper Boundary Response Waveform','FontSize',60)
end
```

pdeconstruction.m

```
% This script is written and read by pdetool and should NOT be edited.
% There are two recommended alternatives:
 % 1) Export the required variables from pdetool and create a MATLAB script
 %    to perform operations on these.
 % 2) Define the problem completely using a MATLAB script. See
 %    http://www.mathworks.com/help/pde/examples/index.html for examples
 %    of this approach.
function pdemodel
[pde_fig,ax]=pdeinit;
pdetool('appl_cb',1);
set(ax,'DataAspectRatio',[1 2.0999999999999996 1]);
set(ax,'PlotBoxAspectRatio',[1 0.66666666666666674 2]);
set(ax,'XLim',[1 2]);
set(ax,'YLim',[-0.20000000000000001 1.2]);
set(ax,'XTick',[ 1,...
 1.1000000000000001,...
 1.2,...
 1.3,...
 1.3999999999999999,...
 1.5,...
 1.6000000000000001,...
 1.7,...
 1.8,...
 1.8999999999999999,...
 2,...
```

```
]);
set(ax,'YTick',[ -0.20000000000000001,...
 -0.10000000000000001,...
 0,...
 0.10000000000000003,...
 0.20000000000000001,...
 0.29999999999999999,...
 0.40000000000000008,...
 0.5,...
 0.59999999999999987,...
 0.69999999999999996,...
 0.79999999999999993,...
 0.89999999999999991,...
 1,...
 1.0999999999999999,...
 1.2,...
]);
pdetool('gridon','on');

% Geometry description:
pderect([1.2 1.8 1.0 0],'R1');
set(findobj(get(pde_fig,'Children'),'Tag','PDEEval'),'String','R1')

% Boundary conditions:
pdetool('changemode',0)
pdesetbd(4,...
'neu',...
1,...
'0',...
'0')
pdesetbd(3,...
'dir',...
1,...
'1',...
'0.125/2*(1+sin(200*pi*t-pi/2))')
pdesetbd(2,...
'neu',...
1,...
'0',...
'0')
pdesetbd(1,...
'neu',...
1,...
```

```
'0',...
'0')

% Mesh generation:
setappdata(pde_fig,'Hgrad',1.3);
setappdata(pde_fig,'refinemethod','regular');
setappdata(pde_fig,'jiggle',char('on','mean',''));
setappdata(pde_fig,'MesherVersion','preR2013a');
pdetool('initmesh')

% PDE coefficients:
pdeseteq(3,...
'8836',...
'0',...
'0',...
'1',...
'0:0.001:0.5',...
'0.0',...
'0.0',...
'[0 100]')
setappdata(pde_fig,'currparam',...
['8836';...
'0   ';...
'0   ';...
'1   '])

% Solve parameters:
setappdata(pde_fig,'solveparam',...
char('0','1000','10','pdeadworst',...
'0.5','longest','0','1E-4','','fixed','Inf'))

% Plotflags and user data strings:
setappdata(pde_fig,'plotflags',[1 1 1 1 1 1 1 0 1 0 1 501 1 0 1 0 0 1]);
setappdata(pde_fig,'colstring','');
setappdata(pde_fig,'arrowstring','');
setappdata(pde_fig,'deformstring','');
setappdata(pde_fig,'heightstring','');

% Solve PDE:
pdetool('solve')
```

PDE Toolbox Mesh

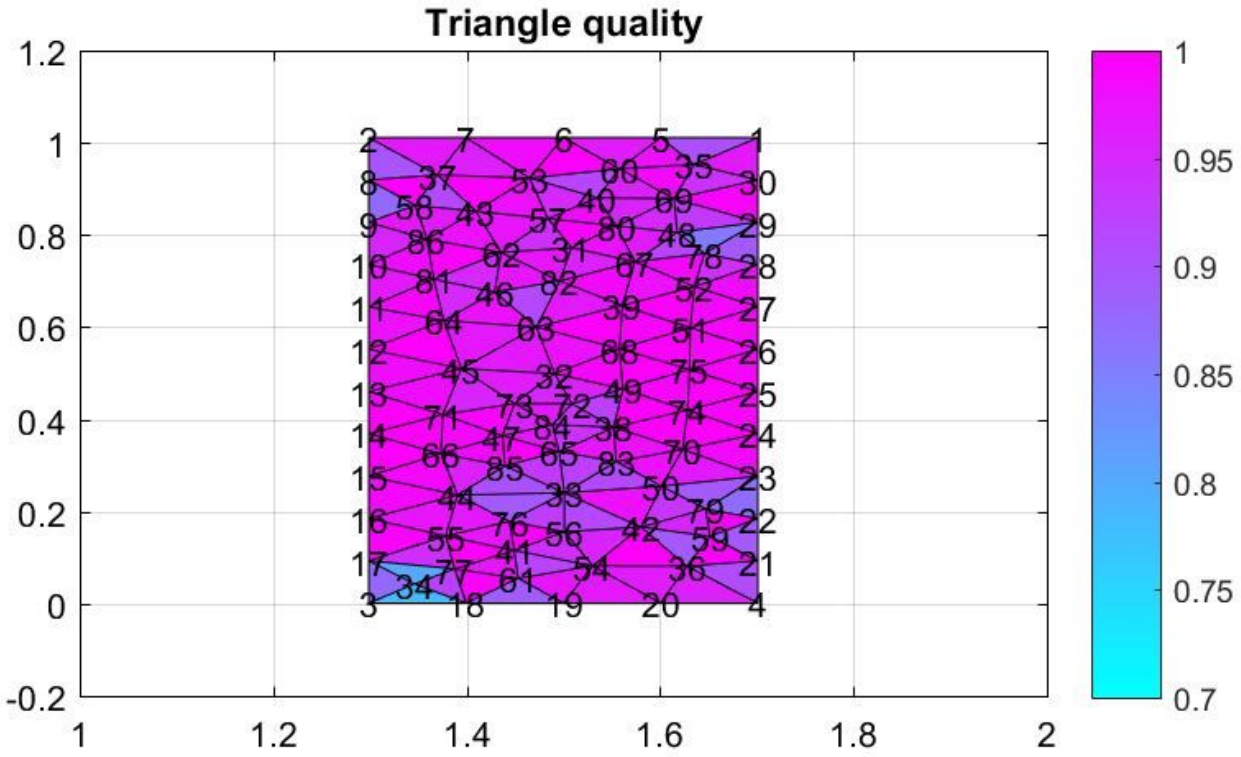
Triangle quality
1.2
1
0.8
0.6
0.4
0.2
0
-0.2
1
1.2
1.4
1.6
1.8
2
1
0.95
0.9
0.85
0.8
0.75
0.7